van Hooff T, Blocken B, 2010. On the effect of wind direction and urban surroundings on natural ventilation of a large semi-enclosed stadium. ***Computers & Fluids*** *39: 1146-55.*

On the effect of wind direction and urban surroundings on natural ventilation of a large semi-enclosed stadium

T. van Hooff [(a,b),1]*, B. Blocken [(a)]

(a) Building Physics and Systems, Eindhoven University of Technology, P.O. box 513, 5600 MB Eindhoven, The Netherlands
(b) Laboratory of Building Physics, Katholieke Universiteit Leuven, Kasteelpark Arenberg 40, 3001 Leuven, Belgium

Abstract

Natural ventilation of buildings refers to the replacement of indoor air with outdoor air due to pressure differences caused by wind and/or buoyancy. It is often expressed in terms of the air change rate per hour (ACH). The pressure differences created by the wind depend – among others – on the wind speed, the wind direction, the configuration of surrounding buildings and the surrounding topography. Computational Fluid Dynamics (CFD) has been used extensively in natural ventilation research. However, most CFD studies were performed for only a limited number of wind directions and/or without considering the urban surroundings. This paper presents isothermal CFD simulations of coupled urban wind flow and indoor natural ventilation to assess the influence of wind direction and urban surroundings on the ACH of a large semi-enclosed stadium. Simulations are performed for eight wind directions and for a computational model with and without the surrounding buildings. CFD solution verification is conducted by performing a grid-sensitivity analysis. CFD validation is performed with on-site wind velocity measurements. The simulated differences in ACH between wind directions can go up to 75% (without surrounding buildings) and 152% (with surrounding buildings). Furthermore, comparing the simulations with and without surrounding buildings showed that neglecting the surroundings can lead to overestimations of the ACH with up to 96%.

Keywords: Natural ventilation; Wind direction; Computational Fluid Dynamics (CFD); Numerical simulation; Model validation; Cross-ventilation

1. Introduction

Environmental awareness and the decreasing availability of fossil fuels have led to an increased interest in more sustainable ways to ensure a healthy and comfortable indoor environment in buildings. Natural ventilation can be an important approach in this respect. It refers to ventilation induced by either wind flow or buoyancy (stack), or a combination of these two driving forces. Whereas natural ventilation is based on natural driving forces, mechanical ventilation uses energy consuming fans to supply air into the building. The feasibility of natural ventilation of buildings depends on several parameters such as the geometry of the building itself, the geometry of the surrounding buildings and the surrounding topography, the wind statistics including prevailing wind direction, etc. Although natural ventilation of buildings has been applied since centuries, it is still an intensive area of research due to both its complexity and its potential for sustainable building design and operation.

A large body of research exists on natural ventilation, based on theory [1-3], analytical work [4-6], experiments [7-10] and numerical simulation with Computational Fluid Dynamics (CFD) [6,7,9,11-19]. CFD has some clear advantages compared to other approaches. Theoretical and analytical approaches are very valuable to provide general insights but are less suitable when complex geometrical configurations are involved. With full-scale (on-site) measurements, many of the influencing parameters (e.g. meteorological conditions) can not be controlled, and the measurements are usually only performed at a few sampling positions. Furthermore, on-site measurements are not an option in the design stage, when the buildings under study have not yet been constructed. Reduced-scale wind tunnel measurements allow controlling the influencing parameters, but the measurements are often only point measurements at a few selected positions. In addition, reduced-scale wind tunnel testing can be hampered by similarity requirements. This is particularly the case for large city models or

[1] Twan van Hooff is a PhD student at both Eindhoven University of Technology and the Katholieke Universiteit Leuven.
* Corresponding author: Twan van Hooff, Building Physics and Systems, Eindhoven University of Technology, P.O. box 513, 5600 MB Eindhoven, the Netherlands. Tel: +31 (0)40 247 5877, Fax: +31 (0)40 243 8595. *E-mail address:* t.a.j.v.hooff@tue.nl

for buildings with small ventilation openings (due to Reynolds number effects), as well as with non-isothermal wind tunnel experiments. The main advantages of CFD are that it allows full control over the influencing parameters and that it provides detailed information on all relevant parameters simultaneously in all points of the computational domain (whole flow-field data). Because the simulations can be performed at full scale, CFD simulations do not suffer from similarity requirements. However, CFD accuracy and reliability are main concerns, and therefore CFD verification and validation studies are imperative.

In spite of the large amount of natural ventilation studies performed in the past, detailed studies on the effect of both wind direction and surrounding buildings on natural ventilation are lacking. This effect is especially important to assess the feasibility of natural ventilation in suburban and urban environments. In such environments, surrounding buildings can provide significant shelter from wind, but could also increase the wind exposure due to channeling effects [20-22]. The influence of the surrounding buildings can be very different depending on the wind direction. Given the disadvantages of experimental approaches, CFD seems the most suitable tool for such investigations. Past computational research efforts in this area could be divided into two categories: (1) studies for isolated buildings, in which the effect of wind direction is due to building geometry and the position of the ventilation openings; and (2) studies for non-isolated buildings, in which the effect of wind direction on natural ventilation is due to the combined effect of surrounding buildings, building geometry and the position of the ventilation openings. Several studies of the first category exist, which have confirmed the large influence of wind direction. Studies of the second category however are rather scarce. A brief overview of studies in each category is given below.

Horan and Finn [15] examined the ACH of a free-standing two-storey naturally ventilated building for four wind directions using CFD and found large variations in ACH between the wind directions, from an ACH value of 3.5 h^{-1} to 15 h^{-1}. More recently, Teitel et al. [16] and Norton et al. [17] performed CFD simulations of natural ventilation in agricultural buildings situated in open terrain. Teitel et al. [16] studied the air flow in one of four clustered greenhouses for four wind directions with an interval of 30° and found significant differences in air flow patterns and ACH (up to 56%). Norton et al. [17] studied the ventilation effectiveness in livestock buildings for wind directions ranging from 0° to 90° with an interval of 10° and found differences in ACH up to 100% depending on the wind direction. Note that all of the aforementioned CFD studies did not consider urban surroundings. Differences in ACH were therefore the result of asymmetry of the building geometry and/or the position of the ventilation openings.

Only a few studies concerning the influence of the building surroundings on natural ventilation and natural ventilation potential are reported in the literature, however most of them are not CFD studies. One example of a CFD study in which a part of the surroundings was included was conducted by Jiang and Chen [18]. They performed Large Eddy Simulations (LES) of fluctuating wind directions to assess the natural ventilation of an apartment in a five-storey high building. The computational domain included nine surrounding buildings in the vicinity of the studied building; other parts of the urban surroundings were not included. This study showed the important influence of short term fluctuations of wind direction within a range of 80° during a short time period of 15 minutes. As opposed to the present study however, it did not consider different steady wind directions. Wirén [23] studied the influence of surrounding buildings on wind pressure distributions and ventilative heat losses in a wind tunnel and found that introducing surrounding buildings changed the measured pressure distributions considerably. The influence of surrounding buildings has also been studied by van Moeseke et al. [24]. However, this study was performed using a software package for the thermal analysis of buildings that includes a 2D CFD module. The package calculated the ACH of the building using pressure coefficients obtained from a parametrical model. It indicated the strong influence of both wind direction and building surroundings. Van Moeseke et al. [24] stressed the unsuitability of parametrical models to accurately assess the wind flow in urban environments, but stated that the method used in their paper might be useful for architects to obtain some first view on the feasibility of natural ventilation. The review paper by Costola et al. [25] on pressure coefficient databases for natural ventilation studies also indicates that very few data exist on the effect of urban surroundings and the related sheltering effects. To the knowledge of the authors, detailed CFD studies on the effect of wind direction and surrounding buildings on indoor natural ventilation in urban environments have not yet been performed.

This paper presents a study on the effect of wind direction and urban surroundings on the natural ventilation of the semi-enclosed *Amsterdam ArenA* stadium in the Netherlands. It is situated in an urban environment with medium to high-rise buildings. Since no HVAC systems are incorporated, natural ventilation is the only means to maintain a healthy and comfortable indoor environment. In a previous study for this stadium, van Hooff and Blocken [19] indicated that the ACH can be insufficient when spectators are present and the stadium roof is closed during summer. Since this previous study focused on the fully coupled outdoor-indoor simulation approach and on the proposed body-fitted grid generation technique, only a few wind directions were studied at that time. In the present paper, the effects of wind direction and urban surroundings on natural ventilation are analyzed in detail. Simulations are performed for eight wind directions using the fully coupled simulation approach, in which outdoor wind flow and indoor air flow are computed simultaneously in the same

computational domain. Furthermore, simulations are performed with and without the surrounding buildings to assess the influence of the surroundings on the ACH. The turbulent wind flow is obtained by solving the 3D steady Reynolds-Averaged Navier-Stokes (RANS) equations in combination with the realizable k-ε turbulence model by Shih et al. [26] and the standard wall functions by Launder and Spalding [27] with roughness modifications by Cebeci and Bradshaw [28]. A grid-sensitivity analysis is performed for CFD solution verification. The CFD model is validated using full-scale wind velocity measurements.

In section 2, the geometry of stadium and surroundings is briefly described. The computational model is outlined in Section 3. Section 4 contains the model validation. The simulation results are given in Section 5. Section 6 (discussion) and Section 7 (conclusions) conclude the paper.

2. Description of stadium and surroundings

The Amsterdam ArenA is a multifunctional dome-shaped stadium with a movable and semi-transparent roof. Fig. 1a shows an aerial view of the stadium with the roof in closed position and Fig. 1b shows a view from street level. Figs. 2a-c provide a detailed plan view and the two cross-sections $\alpha\alpha'$ and $\beta\beta'$. The exterior stadium dimensions are 226 x 190 x 72 m^3 (L x W x H). The stadium has a capacity of 51,628 seated spectators and an interior volume of about 1.2 x 10^6 m^3. The roof can be closed by moving two large panels with a projected horizontal area of 110 x 40 m^2 (L x W). The stadium has four sets of ventilation openings (Fig. 3). The completely opened roof is the largest potential opening (4,400 m²) in the stadium envelope (Fig. 3a). During concerts and other festivities however, which are usually held in the summer period, the roof is closed most of the time to protect the spectators and the technical equipment from wind and rain. When it is closed, natural ventilation of the stadium can only occur through the remaining sets of smaller openings. The second set consists of four large gates in the corners of the stadium (4 x 41.5 m^2), which are connected by an elevated deck (*ArenA deck*) outside the stadium (Fig. 2a and 3b). Each gate has a cross-section L_g x H_g = 6.2 x 6.7 m^2 and can be individually opened and closed. They are open most of the time. The third and fourth sets are two relatively narrow openings in the upper part of the stadium. The first opening is situated between the stand and the steel roof construction, and runs along the entire perimeter of the roof (Fig. 2c (nr.1) and 3c). The total surface area of this opening is 130 m^2. The other opening is situated between the fixed and movable part of the roof (Fig. 2c (nr.2) and 3d). This opening is only present along the two longest edges of the stadium and has a total surface area of about 85 m^2. In the stadium configuration used in this study, the roof is closed, and all other openings are open. Note that the need for higher ventilation rates only occurred in situations with the roof closed [19]. More detailed information on the stadium geometry can be found in [19].

The stadium is located in Amsterdam in the northwest part of the Netherlands. The city and its surroundings are located on very flat terrain; height differences are limited to less than 6 m. The immediate surroundings consist of medium and high rise office buildings (Fig. 4). The height of the surrounding buildings varies from 12 m to a maximum of 95 m for the "ABN-AMRO" office building. The aerodynamic roughness length y_0 of the surroundings, which is needed for the CFD simulations, is determined based on the updated Davenport roughness classification [29] for an upstream fetch of about 10 km. The area on the north side of the ArenA can be classified as "closed terrain" due to the urban character that is present up to a distance of about 10 km upwind. The estimated y_0 for this area is 1.0 m. The terrain south of the ArenA is less rough due to the presence of agricultural and natural areas and can be characterized with an y_0 of 0.5 m. The aerodynamic roughness lengths for the wind directions in this study are summarized in Table 1.

3. Computational model

3.1. Computational geometry and grid

The geometry of the stadium is reproduced in detail using the construction drawings. The very small ventilation openings in the upper part of the stadium (Fig. 3c-d) require details as small as 0.02 m to be modeled. Simulations are made in two computational domains, one for Case 1 without surrounding buildings and one for Case 2, in which the surrounding buildings in a radius of 500 m from the stadium are modeled explicitly, but only by their main shape. In both cases, buildings that are located at a greater distance are modeled implicitly, by imposing an increased equivalent sand-grain roughness height k_S and roughness constant C_S at the bottom of the computational domain. These values are based on the aerodynamic roughness length y_0 of the terrain in and beyond the computational domain and on the relationship between k_S, C_S and y_0 (Eq. 7) for the specific CFD code used in this study, Fluent 6.3.26, which was derived in [30]. The computational domains have dimensions L x W x H = 2,900 x 2,900 x 908.5 m³. The maximum blockage ratio is 1.6%, which is below the recommended maximum of 3% [31,32]. The distance from the building to the sides, to the inlet and to the top of the domain is at least five times the height of the building and the distance from the building to the outlet is fifteen times the height, as recommended by Franke et al. [31] and Tominaga et al. [32].

The quality of the grid in the immediate vicinity of the ventilation openings is considered to be very important for the coupled simulation. Standard automatic or semi-automatic generation of an unstructured grid allows insufficient control of local grid resolution, grid stretching, control volume skewness and aspect ratio. To allow full control over the grid quality and resolution, the grid is constructed using the grid generation procedure presented by van Hooff and Blocken [19]. This procedure allows to efficiently and simultaneously generate the geometry and the computational grid. It consists of a series of extrusion operations, i.e. creating the geometry and the grid based on geometrical translation operations of pre-meshed 2D cross-sections. For more details, the reader is referred to [19]. This procedure allows modeling complex geometries with full control over grid quality and grid resolution. It is executed using the pre-processor Gambit 2.4.6 and results in hybrid grids of hexahedral and prismatic cells. The total number of cells is 5,582,999 for Case 1 and 5,555,949 for Case 2. An overall view of both grids from southwest is shown in Fig. 5, and a more detailed view is given in Fig. 6. Note that the grid refinement at the locations of the absent buildings around the stadium in Fig. 5a is the result of the specific grid generation procedure that is used, enabling the generation of the two different grids from only one basic model by deleting or preserving the meshes volumes at the building locations [19].

A grid-sensitivity analysis is performed by conducting simulations on a coarser grid with 3.0 million cells and a finer grid with 9.2 million cells. The three grids are compared based on the mass flow rates through the four gates, which are the main ventilation openings for the situation with closed roof. The difference in normalized mass flow rates between the coarse grid and the middle grid is 4.7%, whereas the difference between the middle grid and the fine grid is only 2.0%. Therefore, the middle grid was selected for further analysis.

3.2. Boundary conditions and solver settings

At the inlet of the domain, a logarithmic mean wind speed profile representing a neutral atmospheric boundary layer is imposed with y_0 = 0.5 m or 1.0 m, depending on the wind direction (see Table 1), and a reference wind speed U_{10} (at 10 m height) of 5 m/s. For y_0 = 0.5 m, the inlet longitudinal turbulence intensity I_U ranges from 30 % at pedestrian height (y = 2 m) to 5 % at gradient height. For y_0 = 1 m, I_U ranges from 40 % (y = 2 m) to 8% at gradient height. Turbulent kinetic energy k is calculated from I_u and U assuming isotropic turbulence:

$$k = 1.5(I_U U)^2 \tag{1}$$

The turbulence dissipation rate ε is calculated as:

$$\varepsilon = \frac{(u^*_{ABL})^3}{\kappa(y + y_0)} \tag{2}$$

where y is the height coordinate, κ the von Karman constant (κ = 0.42) and u_{ABL}* the atmospheric boundary layer (ABL) friction velocity related to the logarithmic mean wind speed profile. Figure 7 shows the resulting vertical profiles of mean wind speed, turbulent kinetic energy and turbulence dissipation rate.

The standard wall functions by Launder and Spalding [27] are used with the sand-grain based roughness modification by Cebeci and Bradshaw [28]. The velocity wall function in the CFD code is implemented as [33]:

$$\frac{U_P u^*}{u_\tau} = \frac{1}{\kappa}\ln\left(E\frac{u^* y_P}{\nu}\right) - \Delta B \tag{3}$$

where y_P is the distance between the centre point P of the wall-adjacent cell and the wall, U_P is the tangential wind speed in point P, E is the empirical constant for a smooth wall (≈ 9.793), ν is the kinematic viscosity of the fluid, ΔB is the roughness function and u^* and u_τ are the wall-function friction velocities defined as:

$$u^* = C_\mu^{1/4} k_P^{1/2} . \tag{4}$$

$$u_\tau = \sqrt{\frac{\tau_w}{\rho}} \tag{5}$$

where C_μ is a model constant (0.09), k_P is the turbulent kinetic energy in point P, τ_w is the wall shear stress and ρ is the density of the fluid. In the fully rough regime ΔB is given by:

$$\Delta B = \frac{1}{\kappa}\ln\left(1 + C_S k_S^+\right) \tag{6}$$

where k_S^+ is the nondimensional roughness height: $k_S^+ = k_S u^*/\nu$. The parameters k_S and C_S in the roughness modification are determined from their appropriate relationship with y_0. This relationship was derived by Blocken et al. [30] for Fluent and CFX. For Fluent 6, up to at least version 6.3, it is given by:

$$k_S = \frac{9.793\, y_0}{C_S} \tag{7}$$

Note that Fluent 6 (up to at least version 6.3) does not allow k_S to be larger than y_P. If the user implements a larger value, the code will automatically set k_S equal to y_P without warning. Therefore, in this study, k_S is taken smaller than or equal to y_P and C_S is chosen to satisfy Eq. (7). A user-defined function setting the value of the constant C_S is required because the Fluent 6.3 code does not allow it to exceed the interval [0;1] otherwise. For the ground surface with implicitly modeled buildings, k_S is taken 0.7 m and $C_S = 7$ for $y_0 = 0.5$ m. For $y_0 = 1.0$ m, $k_S = 1.4$ m and $C_S = 7$. For the ground surface in the direct vicinity around the explicitly modeled buildings and the stadium, $y_0 = 0.03$ m is taken, which is imposed by setting $k_S = 0.59$ m and $C_S = 0.5$. The building surfaces are set to have zero roughness height ($k_S = 0$). This choice is based on parametric CFD studies with k_S values of 0, 0.01 m and 0.05 m, which showed no notable differences for the ventilation flow rates, and which can be explained by the pressure drag being much larger than the friction drag over the stadium. The top of the computational domain is modeled as a slip wall (zero normal velocity and zero normal gradients of all variables) and zero static pressure is imposed at the outlet. Only isothermal simulations are performed in this study, in line with the neutral atmospheric stratification during the wind velocity measurements, which were performed on days with strong winds and cloudy conditions.

The CFD code Fluent 6.3.26 [33] is used to solve the 3D steady RANS equations. Closure of the RANS equations is obtained with the realizable k-ε turbulence model [26]. The SIMPLE algorithm is used for pressure-velocity coupling, pressure interpolation is standard and second order discretization schemes are used for both the convection terms and the viscous terms of the governing equations. A Sun Fire X4150 server containing two Quad-Core Intel Xeon E5440 2.83 GHz processors and 16 GB Fully Buffered DDR2 memory was used to perform the simulations. Every simulation reached convergence after about 20 hours of wall clock time in which 6000 iterations were performed. The scaled residuals [33] reached the following minimum values: 10^{-7} for x, y and z velocity, 10^{-6} for k and ε, and 10^{-5} for continuity.

4. Validation with full-scale wind velocity measurements

4.1. Measurements

For CFD validation purposes, the 3D wind velocity in and around the stadium was measured on days with neutral atmospheric stratification (strong winds (reference wind speed U_{ref} above 8 m/s) and cloudy conditions) in the period September-November 2007. The measurements were performed with ultrasonic anemometers, positioned on mobile posts, at 2 m height above the ArenA deck (Fig. 6) in the four gates which are the main ventilation openings when the roof is closed. The reference wind speed (U_{ref}) was measured on top of a 10 m mast on the roof of the 95 m high ABN-AMRO office building, which is the highest building in the proximity of the stadium (Fig. 3). The measurement data were sampled at 5 Hz, averaged into 10-minute values and analyzed. Only data with at least 12 different 10-minute values per wind direction sector of 10° were retained in order to obtain adequate averaged wind velocities and standard deviations. The measured wind speed U in the four gates was divided by the reference wind speed U_{ref} measured on top of the ABN-AMRO office building. Note that the term "wind speed" here refers to the magnitude of the 3D mean wind velocity vector.

4.2. Comparison measurements and CFD

The computational model is validated using the 3D velocity measurements. The wind speed ratio U/U_{ref} is also calculated with CFD and both ratios are compared. The same comparison is made for the measured and calculated local wind directions at the stadium measurement positions. Fig. 8a compares simulated and measured mean wind speed ratios for $\varphi = 228^\circ$ and a closed roof, indicating a rather good agreement. The simulations show that significant wind speed gradients exist at measurement position D. As a result, a small shift in measurement position or a small change in the flow field can significantly affect the simulation values at this position. To indicate this effect, the deviations in simulated wind speed by a 0.5 m shift in position are indicated by "error bars". Note however that in most cases, the gradients are too small for the error bars to be visible. A

good agreement between measurements and simulations is also found for the local wind direction in the gates (Fig. 8b), except for gate D, where a deviation of 30% is found. Overall, a fair to good agreement is obtained in this validation study, and the stadium model is used to assess the influence of wind direction and urban surroundings on natural ventilation.

5. Results

The validated CFD model is used to perform simulations for eight wind directions, for the situation without (Case 1) and with surrounding buildings (Case 2). Both sets of simulations are conducted for a reference wind speed U_{10} at 10 m height of 5 m/s. The eight wind directions are φ = 16°, 61°, 106°, 151°, 196°, 241°, 286° and 331°, all perpendicular or with an angle of 45° to the symmetry axis of the stadium as indicated in Figure 9a. Natural ventilation is evaluated based on the ACH, which is the amount of air that enters a room during a certain time period, divided by the interior volume of the same room [34], and can be calculated by:

$$ACH = \frac{Q \cdot 3600}{V} \tag{8}$$

where the unit of ACH is h^{-1}, Q is the volumetric air flow rate into the enclosure (m^3/s) and V the volume of the enclosure (m^3). For each simulation, the mass flow rates through each opening are used to calculate Q. The parameter ACH/U_{10} (s/mh) is used in this study because the results are independent of U_{10}. This was demonstrated by performing test simulations at a few other reference wind speeds. Note that both hours and seconds are present in the unit of the ACH/U_{10}. It was chosen to maintain these two units for time since the definition of ACH is air changes per hour and the standard notation for wind speed is m/s.

5.1. Case 1

The surrounding buildings within a radius of 500 m are not included in this case (Fig. 5a), while the buildings that are situated at a larger distance are modeled implicitly by imposing the appropriate equivalent sand-grain roughness height k_S and roughness constant C_S at the bottom of the domain. The results of these simulations are shown in Figure 9b. The calculated ACH/U_{10} lies around 0.25 s/mh with small deviations for most wind directions, but a significantly larger deviation is present for φ = 16° (ACH/U_{10} = 0.35 s/mh). These deviations can be attributed to two reasons. The first is the asymmetry of the stadium as shown in Figure 9a. The geometrical differences are mainly present at the ArenA deck, i.e. at the same height as the location of the gates (Fig. 3b). As mentioned in Section 2, the gates are the largest ventilation openings present when the roof is closed. Deviations in air flow in the proximity of these gates can therefore result in a relatively large variation in ACH. The second, but less important, reason is the variation of the aerodynamic roughness length y_0 from 0.5 m to 1.0 m depending on the wind direction (see Table 1).

5.2. Case 2

The simulations described in section 5.1 are repeated, but this time with explicit modeling of the surrounding buildings (Fig. 10a). The aerodynamic roughness lengths y_0 are that the same as in Case 1. The results of the calculations are shown in Figure 10b and demonstrate the strong dependence of ACH/U_{10} on wind direction when surrounding buildings are present. For example, the value of ACH/U_{10} for φ = 16° (0.35 s/mh) is 2.5 times as high as for φ = 196° (0.14 s/mh). The results between other wind directions also show larger deviations than for Case 1. The lower ACH for φ = 196º can be explained by the presence of a group of large buildings upstream of the stadium. These buildings provide some shelter from wind. Figure 11 shows the contours of the ratio U/U_{10} around the stadium for four wind directions (φ = 16°, 106°, 196° and 286°) in a horizontal plane at a height of 8 m above the ArenA deck. For φ = 196° the stadium is in the wake of the high-rise buildings that are present upstream, resulting in lower velocities and pressures near the windward ventilation openings. For the other three wind directions the influence of the surrounding buildings on the velocity near the stadium is less pronounced. Figure 12 shows that the prevailing wind direction at the site is southwest, which is also the wind direction for which shelter by the urban surroundings is most pronounced. This stresses the importance, especially for this case, of performing CFD simulations for a range of wind directions for an accurate assessment of the ACH.

5.3. Case 1 versus Case 2

Figure 13 provides an overview of the ACH/U_{10} values obtained from CFD simulations with and without the stadium surroundings. The largest differences occur for wind direction φ = 196°. The ACH for this wind direction is overestimated by 96% when the natural ventilation of the stadium would be assessed without the

surrounding buildings in the CFD model. For wind directions of 16° and 286°, without any large buildings present upstream, the differences in ACH/U_{10} are negligible. It appears that, at least in this case, the channeling effects between the stadium and the surrounding buildings are not strong enough to influence the ACH.

6. Discussion

In this study the influence of wind direction and urban surroundings on the air exchange rate of a large multifunctional stadium has been assessed using CFD simulations. Some limitations of this study and needs for further research are mentioned below.

Firstly, only steady-state CFD simulations were performed in this study. In a next stage, transient CFD simulations will be performed to study the influence of pulsating flow and large eddies on the air exchange between the building interior and the external wind flow. Although the validation study showed a good agreement between the measurements and the RANS simulations, future research will compare the air exchange rates obtained with steady RANS simulations with those from transient simulations with Large Eddy Simulation (LES) and/or Detached Eddy Simulation (DES). Secondly, only isothermal simulations were performed in this study, although a previous study [19] indicated the strong influence that local buoyancy, as a result of higher temperatures inside the stadium compared to the ambient air temperature, can have on the ACH. Note that both in the previous and in the current study, a neutral atmospheric boundary layer was assumed. The decision to focus on only isothermal simulations in the present study was made to limit the number of influencing parameters in order to provide some first insights in the influence of wind direction and urban surroundings on the ACH. Thermal simulations would increase the complexity of the flow field considerably. Furthermore, thermal simulations would require conducting simulations at different reference wind speeds U_{10}, because the ACH can not be scaled linearly with U_{10} anymore. Future studies will focus on the influence of wind direction and urban surroundings in thermal simulations. In general, the interaction between wind and buoyancy as driving forces for natural ventilation is an important topic of future research.

7. Conclusions

A study on the influence of wind direction and urban surroundings on natural ventilation of a large semi-enclosed stadium has been presented in this paper. The 3D steady RANS CFD simulations are performed isothermally (no buoyancy) and in a coupled way, i.e. the outdoor and the indoor air flow are solved simultaneously and within the same computational domain. The high-resolution body-fitted grid was based on a grid-sensitivity analysis, indicating the 5.6 million cell hybrid grid to be adequate for this study. The CFD model was validated using on-site full-scale 3D wind velocity measurements in the four gates of the stadium. An overall to good agreement was obtained between CFD simulations and measurements.

The natural ventilation (air change rate per hour – ACH) was assessed for eight wind directions and for two cases: with and without surrounding buildings. The results of both cases have demonstrated the importance of performing simulations with a range of wind directions. For the isolated stadium (without surrounding buildings), the differences between two wind directions can be as large as 75%. For the stadium in its urban environment, the differences between two wind directions can go up to 152%. Furthermore, this study has shown the need to model the surrounding urban environment for natural ventilation analysis. Excluding the urban environment in the computational domain can lead to an overestimation of the ACH with 96%. While disregarding surrounding buildings and focusing on only a limited number of wind directions can be sufficient for isolated buildings and/or buildings in a rural environment, this can give very large errors for buildings in suburban and urban areas.

Acknowledgements

The measurements reported in this paper were supported by the Laboratory of the Unit Building Physics and Systems (BPS) of Eindhoven University of Technology. Special thanks go to Ing. Jan Diepens, head of LBPS, and Ing. Harrie Smulders, Wout van Bommel and GeertJan Maas, members of the LBPS, for their important contribution. We also thank Martin Wielaart, manager at the Amsterdam ArenA for his help during the measurements.

References

[1] Awbi HB. Ventilation of buildings. London, Spon Press; 1991.
[2] Awbi HB. Design considerations for naturally ventilated buildings. Renew Energ 1994;5:1081-90.
[3] Etheridge D, Sandberg M. Building Ventilation: Theory and Measurement, Wiley, Chichester, England; 1996.

[4] Linden PF. The fluid mechanics of natural ventilation. Annu Rev Fluid Mech 1999;31:201-38.
[5] Coffey CJ, Hunt GR. Ventilation effectiveness measures based on heat removal: Part 2. Application to natural ventilation flows. Build Environ 2007;42(6):2249-62.
[6] Ji Y, Cook MJ, Hanby V. CFD modelling of natural displacement ventilation in an enclosure connected to an atrium. Build Environ 2007;42(3):1158-72.
[7] Straw MP, Baker CJ, Robertson AP. Experimental measurements and computations of the wind-induced ventilation of a cubic structure. J Wind Eng Ind Aerodyn 2000;88(2-3):213-30.
[8] Ohba M, Irie K, Kurabuchi T. Study on airflow characteristics inside and outside a cross-ventilation model, and ventilation flow rates using wind tunnel experiments. J Wind Eng Ind Aerodyn 2001;89(14-15):1513-24.
[9] Jiang Y, Alexander D, Jenkins H, Arthur R, Chen Q. Natural ventilation in buildings: Measurement in a wind tunnel and numerical simulation with large-eddy simulation. J Wind Eng Ind Aerodyn 2003;91(3): 331-53.
[10] Karava P, Stathopoulos T, Athienitis AK. Wind-induced natural ventilation analysis. Sol Energy 2007;81(1):20-30.
[11] Cook MJ, Ji Y, Hunt GR. CFD modeling of natural ventilation: combined wind and buoyancy forces. Int J Vent 2003;1(3):169-80.
[12] Wright NG, Hargreaves DM. Unsteady CFD Simulations for natural ventilation. Int J Vent 2006;5(1):13-20.
[13] Yang T, Wright NG, Etheridge DW, Quinn AD. A comparison of CFD and full-scale measurements for analysis of natural ventilation. Int J Vent 2006;4(4):337-48.
[14] Hu C-H, Ohba M, Yoshie R. CFD modelling of unsteady cross ventilation flows using LES. J Wind Eng Ind Aerodyn 2008;96(10-11):1692-1706.
[15] Horan JM, Finn DP. Sensitivity of air change rates in a naturally ventilated atrium space subject to variations in external wind speed and direction. Energy Build 2008;40(8):1577-85.
[16] Teitel M, Ziskind G, Liran O, Dubovsky V, Letan R. Effect of wind direction on greenhouse ventilation rate, airflow patterns and temperature distributions. Biosystems Eng 2008;101(3):351-69.
[17] Norton T, Grant J, Fallon R, Sun D-W. Assessing the ventilation effectiveness of naturally ventilated livestock buildings under wind dominated conditions using computational fluid dynamics. Biosystems Eng 2009;103(1):78-99.
[18] Jiang Y, Chen Q. Effect of fluctuating wind direction on cross natural ventilation in buildings from large eddy simulation. Build Environ 2002;37(4):379-86.
[19] Van Hooff T, Blocken B. Coupled urban wind flow and indoor natural ventilation modelling on a high-resolution grid: A case study for the Amsterdam ArenA stadium. Environ Modell Softw 2010;25(1):51-65.
[20] Blocken B, Carmeliet J, Stathopoulos T. CFD evaluation of the wind speed conditions in passages between buildings – effect of wall-function roughness modifications on the atmospheric boundary layer flow. J Wind Eng Ind Aerodyn 2007:95(9-11):941-62.
[21] Blocken B, Stathopoulos T, Carmeliet J. Wind environmental conditions in passages between two long narrow perpendicular buildings. J. Aerosp. Eng.– ASCE 2008:21(4):280-87.
[22] Blocken B, Moonen P, Stathopoulos T, Carmeliet J. A numerical study on the existence of the Venturi-effect in passages between perpendicular buildings. J. Eng. Mech. – ASCE 2008:134(12):1021-28.
[23] Wirén BG. Effects of surrounding buildings on wind pressure distributions and ventilative heat losses for a single-family house. J Wind Eng Ind Aerodyn 1983;15(1-3):15-26.
[24] Van Moeseke G, Gratia E, Reiter S, De Herde A. Wind pressure distribution influence on natural ventilation for different incidences and environment densities. Energy Build 2005;37(8):878-89.
[25] Costola D, Blocken B, Hensen JLM. Overview of pressure coefficient data in building energy simulation and airflow network programs. Build Environ 2009;44(10): 2027-36.
[26] Shih T-H, Liou WW, Shabbir A, Zhu J. A new k-e eddy-viscosity model for high Reynolds number turbulent flows—model development and validation. Comput Fluids 1995;24(3):227–38.
[27] Launder BE, Spalding DB. The numerical computation of turbulent flows. Comp Methods Appl Mech Eng 1974;3:269-89.
[28] Cebeci T, Bradshaw P. Momentum transfer in boundary layers, Hemisphere Publishing Corporation; 1977.
[29] Wieringa J. Updating the Davenport roughness classification. J Wind Eng Ind Aerodyn 1992;41(1):357-68.
[30] Blocken B, Stathopoulos T, Carmeliet J. CFD simulation of the atmospheric boundary layer: wall function problems. Atmos Environ 2007;41(2):238-52.
[31] Franke J, Hellsten A, Schlünzen H, Carissimo B (Eds.). Best practice guideline for the CFD simulation of flows in the urban environment. COST Office Brussels, 2007.
[32] Tominaga Y, Mochida A, Yoshie R, Kataoka H, Nozu T, Yoshikawa M, Shirasawa T. AIJ guidelines for practical applications of CFD to pedestrian wind environment around buildings. J Wind Eng Ind Aerodyn 2008;96(10-11):1749-61.

[33] Fluent Inc. Fluent 6.3 User's Guide. Fluent Inc., Lebanon; 2006.
[34] ASHRAE. Handbook of Fundamentals. American Society of Heating, Refrigerating and Air-Conditioning Engineers, Inc., Atlanta, USA; 2005.
[35] NEN. Application of mean hourly wind speed statistics for the Netherlands, NPR 6097:2006 (in Dutch). Dutch Practice Guideline; 2006.

FIGURES

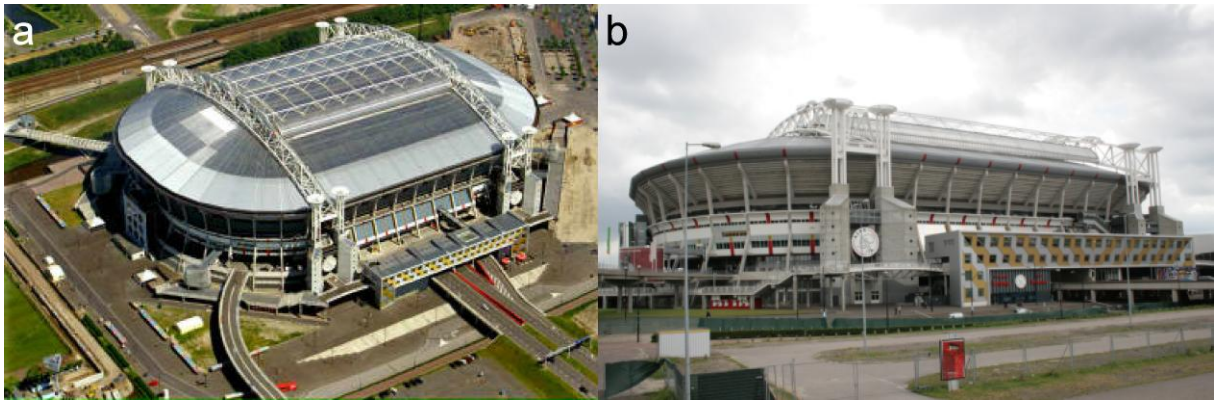

Fig. 1. Amsterdam ArenA stadium. (a) Aerial view from northwest of the stadium with the roof closed; (b) street view of the stadium from northwest.

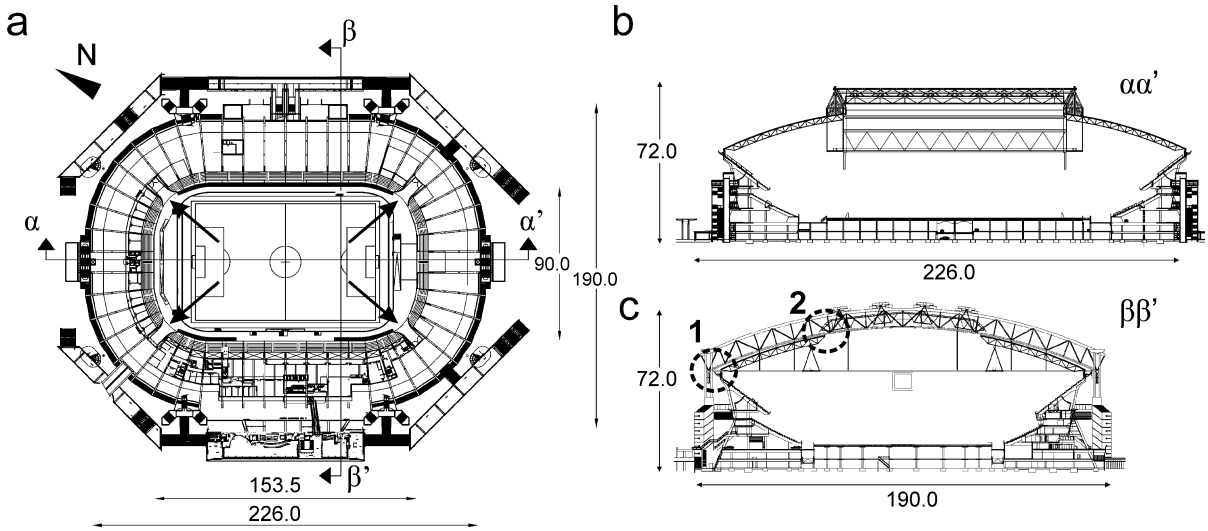

Fig. 2. (a) Horizontal cross-section at a height of 2 m above the deck, which is situated at 8.5 m above ground level. The four arrows indicate the location of the openings in the corners of the stadium (gates), (b) vertical cross-section αα'; (c) vertical cross-section ββ'. The dashed circles show the positions of the ventilation openings in the upper part of the stadium. Dimensions in m.

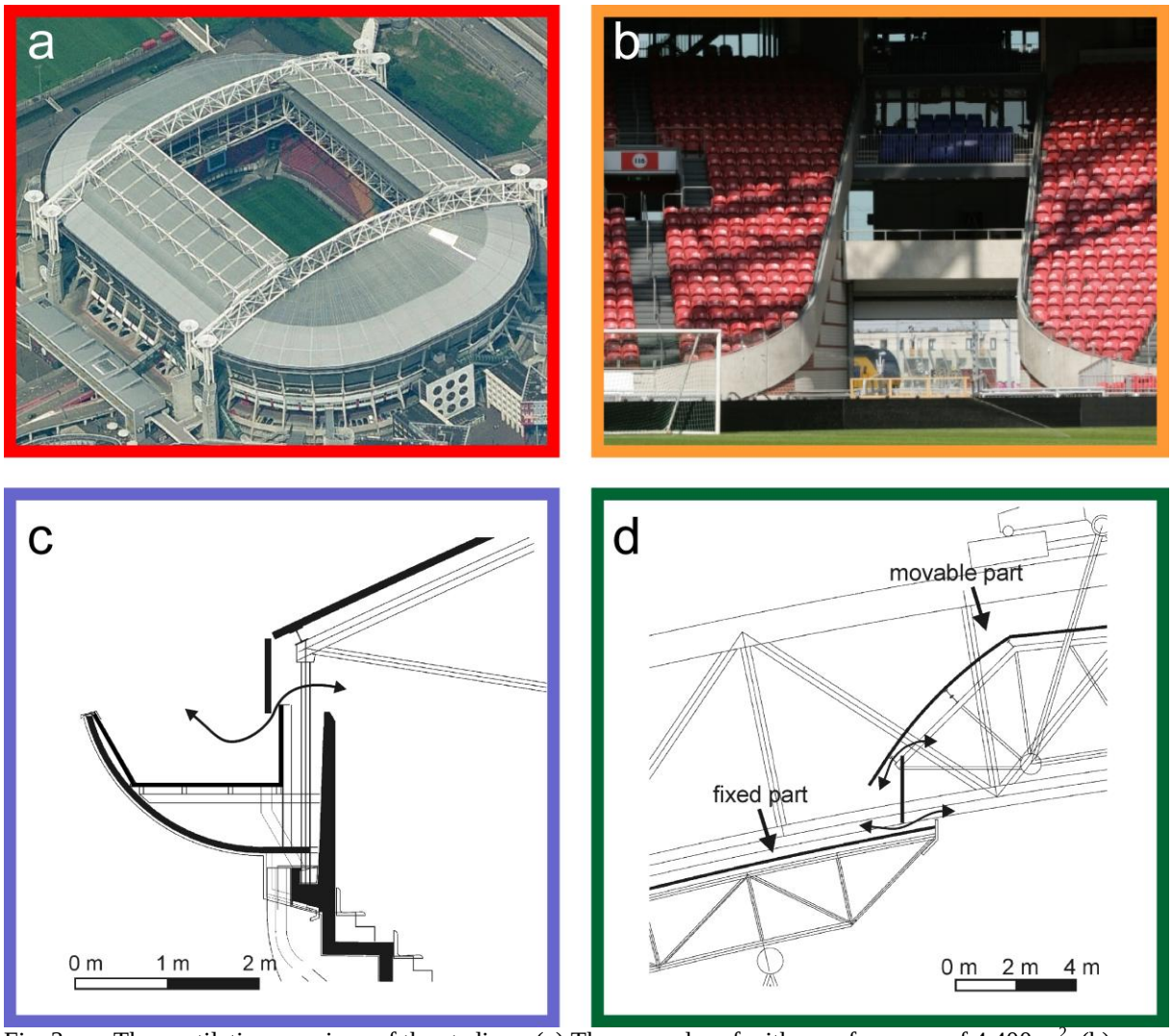

Fig. 3. The ventilation openings of the stadium; (a) The opened roof with a surface area of 4,400 m^2; (b) one of the four openings in the corner of the stadium (gates) (166 m^2); (c) ventilation opening between the steel roof construction, the gutter and the concrete stand (Fig. 2c; nr. 1) (130 m^2); (d) ventilation opening between the fixed and movable part of the roof (85 m^2) (Fig. 2c; nr. 2).

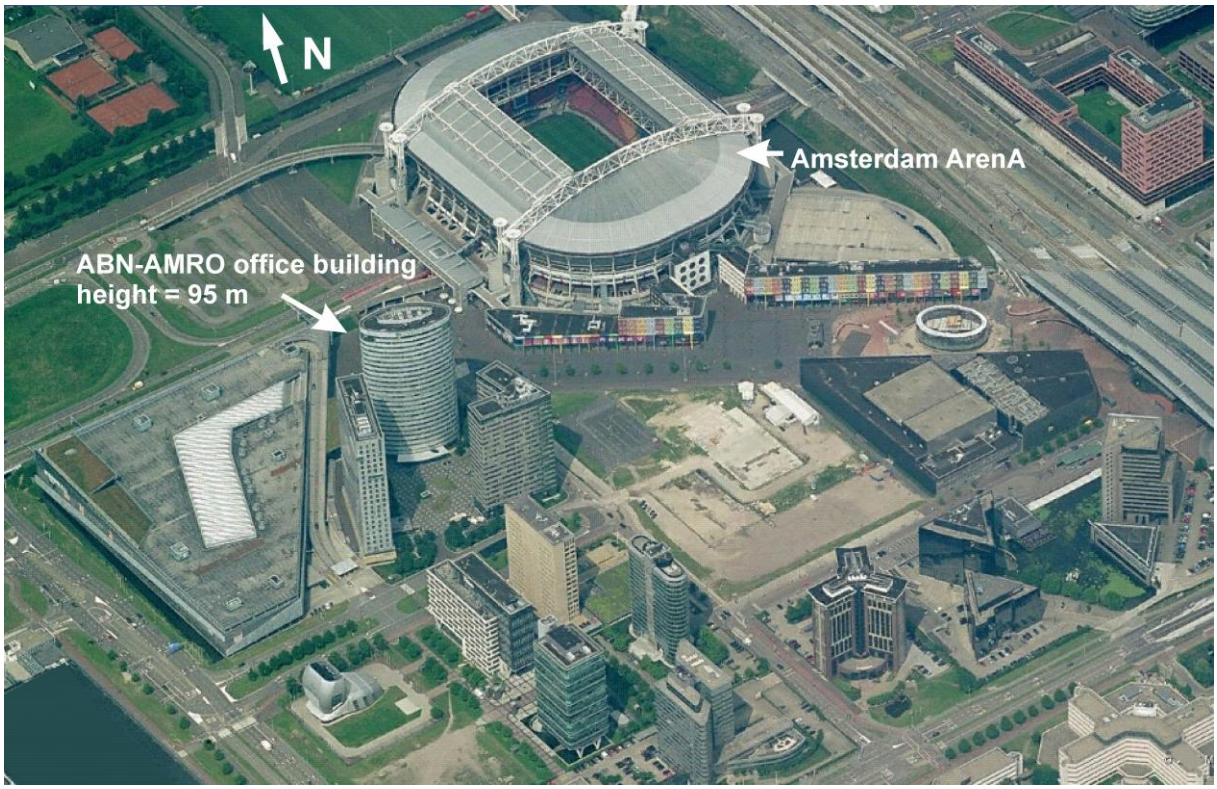

Fig. 4. Aerial view from southwest of the Amsterdam ArenA football stadium and surroundings. The 95 m high ABN-AMRO tower is indicated.

a

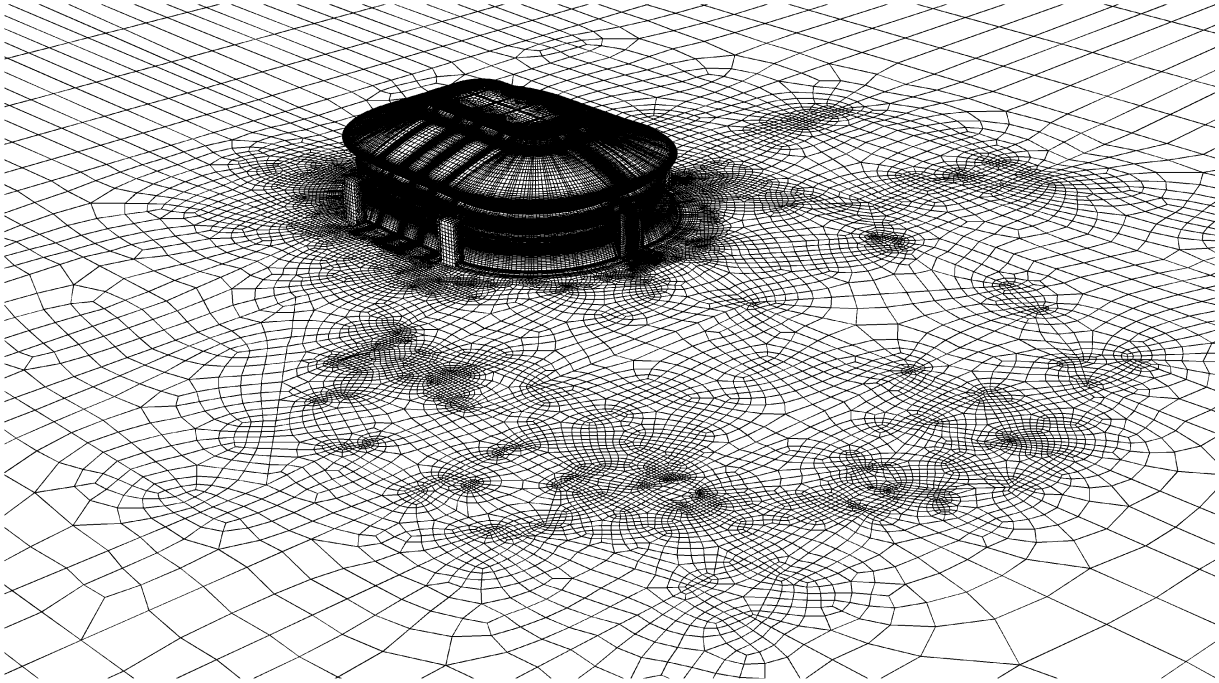

b

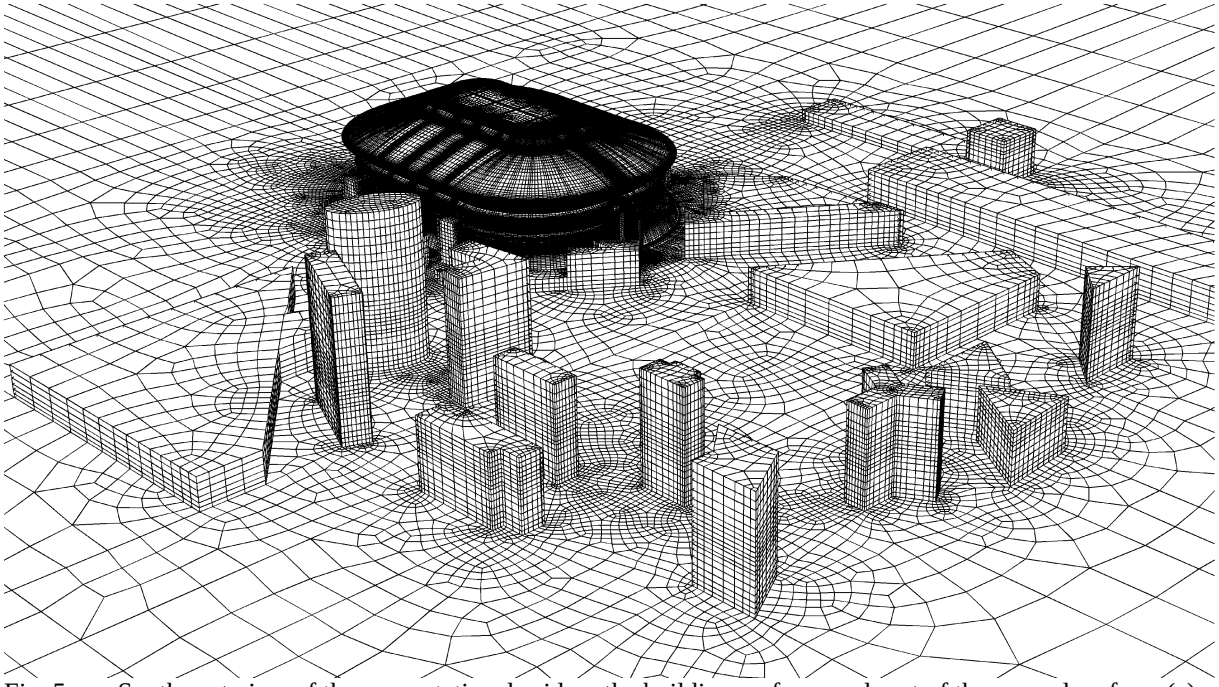

Fig. 5. Southwest view of the computational grid on the building surfaces and part of the ground surface. (a) Case 1: without surrounding buildings; (b) Case 2: with surrounding buildings. Note that the grid refinement at the locations of the absent buildings around the stadium in Fig. 5a is the result of the specific grid generation procedure that is used, enabling the generation of the two different grids from only one basic model [19].

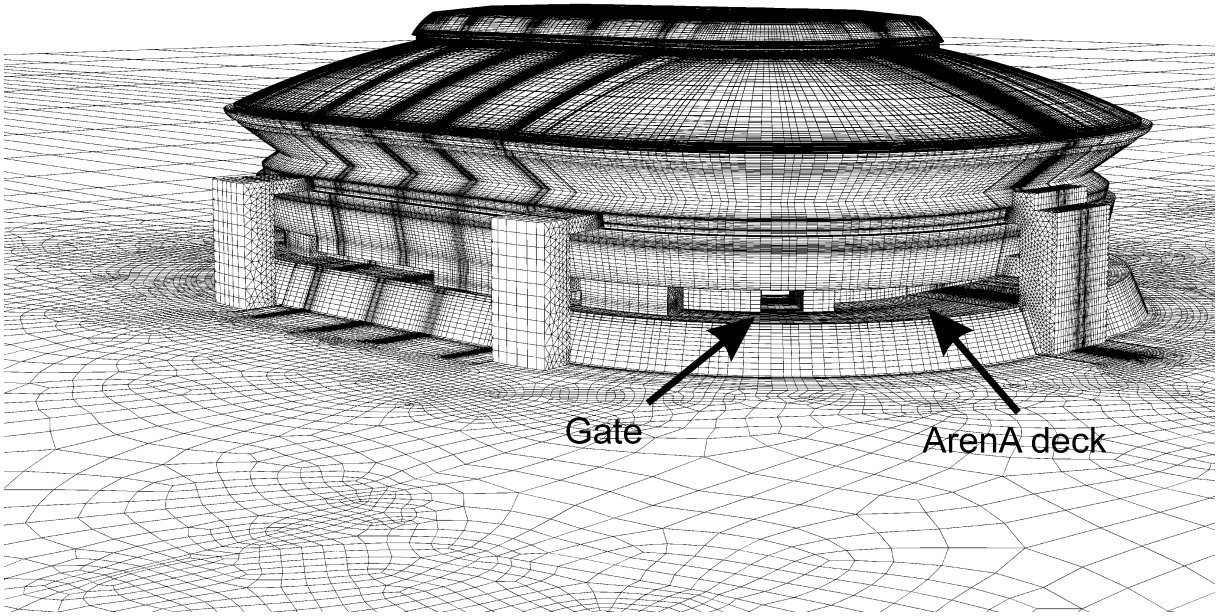

Fig. 6. Southwest view of the grid for the case without surrounding buildings, illustrating details such as one of the four openings (gates) in the corner of the stadium.

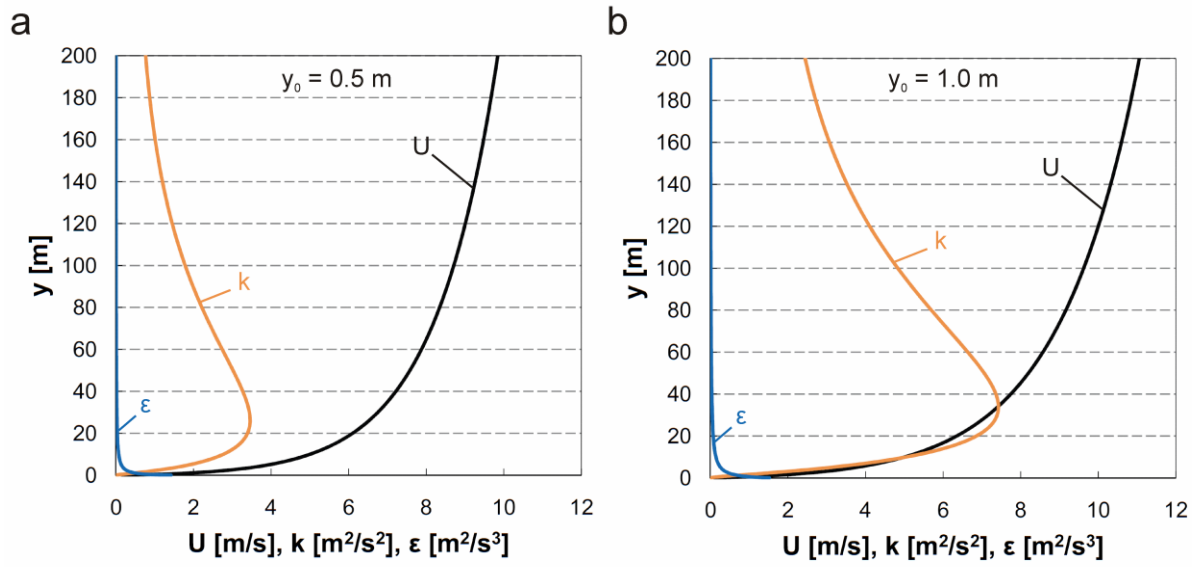

Fig. 7. Inlet profiles of mean wind speed U, turbulent kinetic energy k and turbulence dissipation rate ε for (a) y_0 = 0.5 m; (b) y_0 = 1 m.

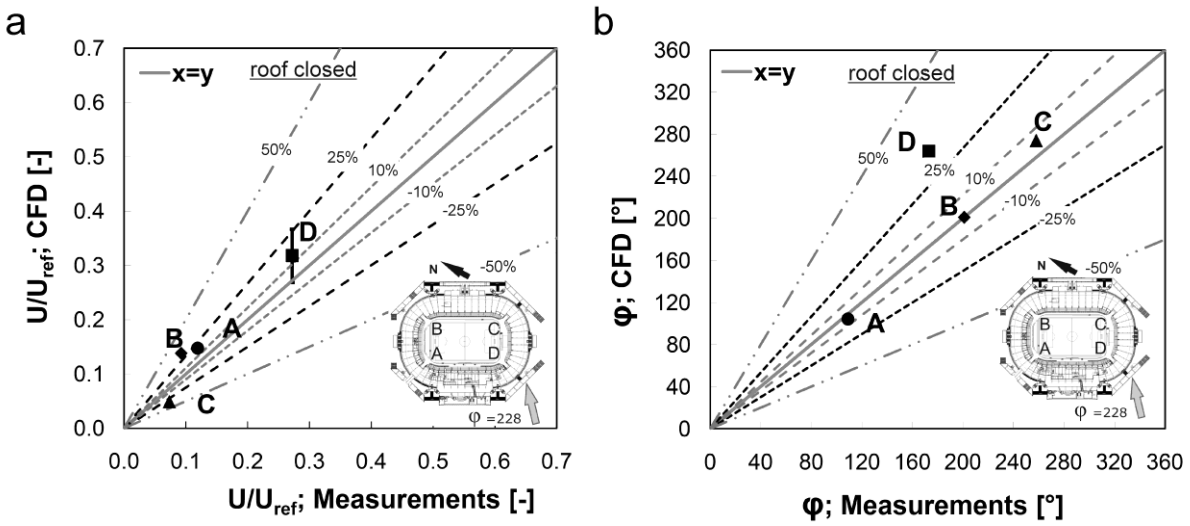

Fig. 8. Comparison between numerical and experimental results in the four gates A, B, C and D, for closed roof and wind direction of 228º: (a) non-dimensional velocity magnitude U/U_{ref}; (b) wind direction φ. The error bars are a measure of the local spatial gradients in the CFD simulation. The percentages indicate the deviation between the measurements and the CFD simulations.

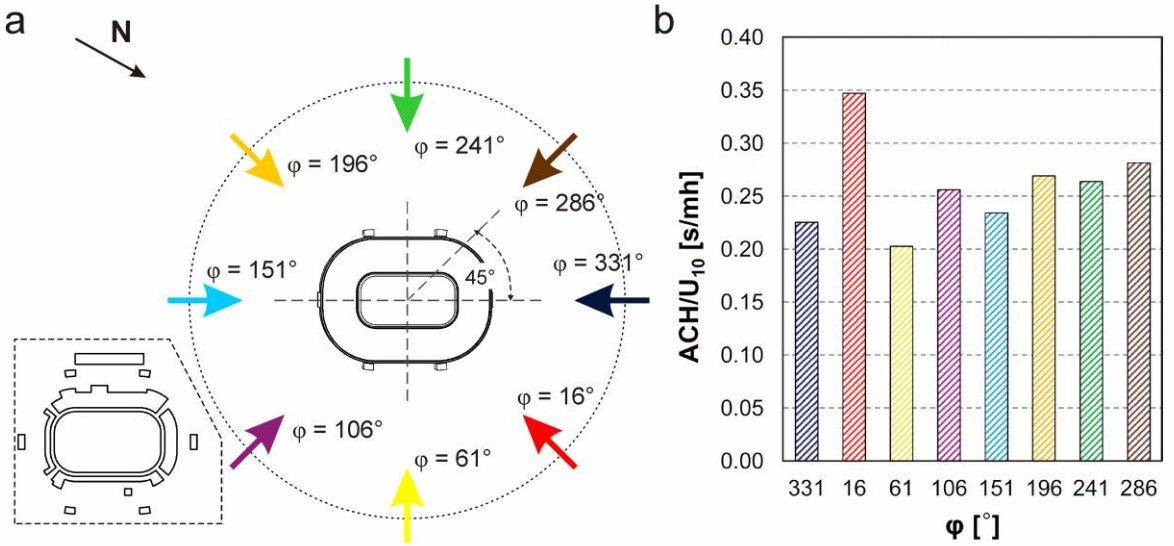

Fig. 9. (a) Top view of stadium without surrounding buildings, with indication of wind directions for the CFD simulations. The figure in the left bottom corner shows a horizontal cross-section taken at 2 m above the ArenA deck, indicating the asymmetry of the stadium. (b) Ratio of air change rate ACH to reference wind speed U_{10} (s/mh) for the wind directions in Fig. 9a.

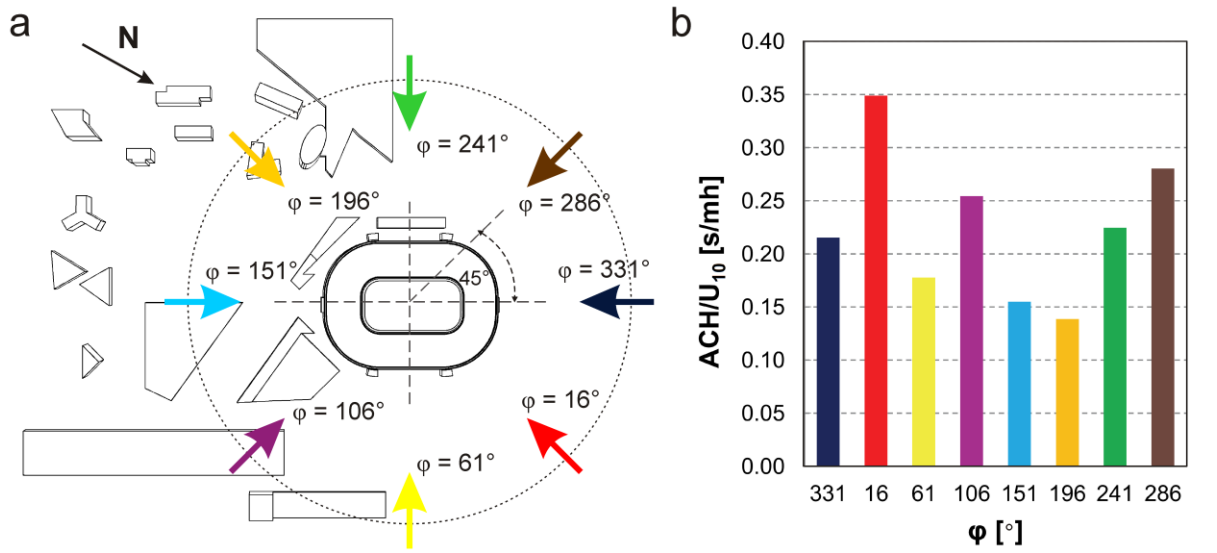

Fig. 10. (a) Top view of stadium and surrounding buildings with indication of wind directions for the CFD simulations. (b) Ratio of ACH to U_{10} (s/mh) for the wind directions in Fig. 10a.

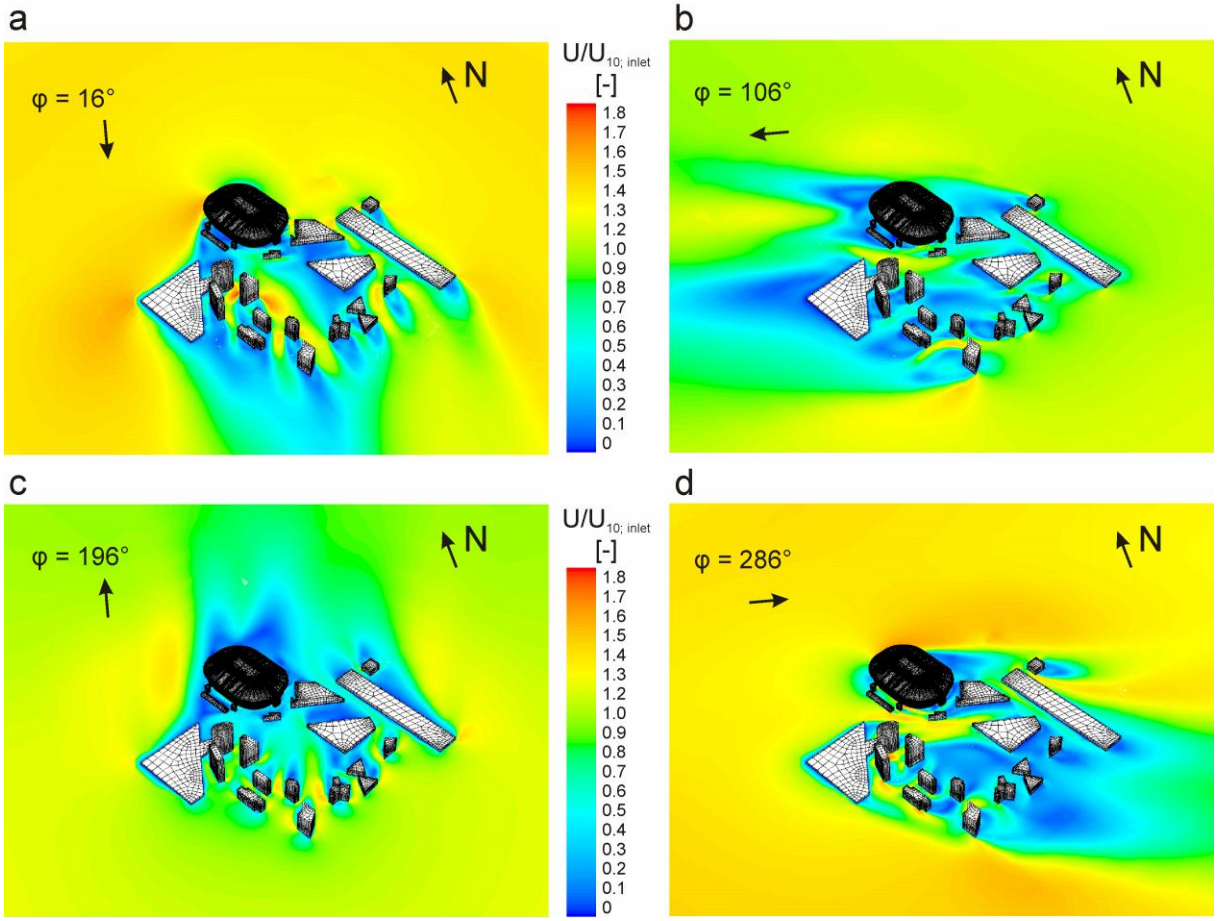

Fig. 11. Contours of non-dimensional velocity magnitude U/U_{10} in a horizontal plane at 8 m height above the ArenA deck for U_{10} = 5 m/s and for (a) φ = 16°; (b) φ = 106°; (c) φ = 196°; (d) φ = 286°. For φ = 196°, the stadium is situated in the wake of the high-rise surrounding buildings, yielding lower U/U_{10} and a lower ACH for this wind direction.

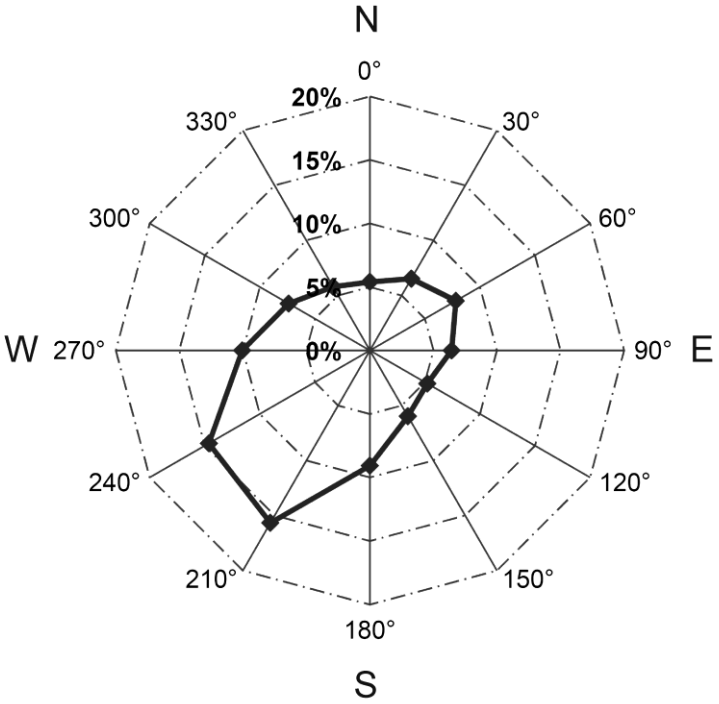

Fig. 12. Wind direction statistics (60 m height) at the building site, indicating that the prevailing wind direction is southwest (based on [35]).

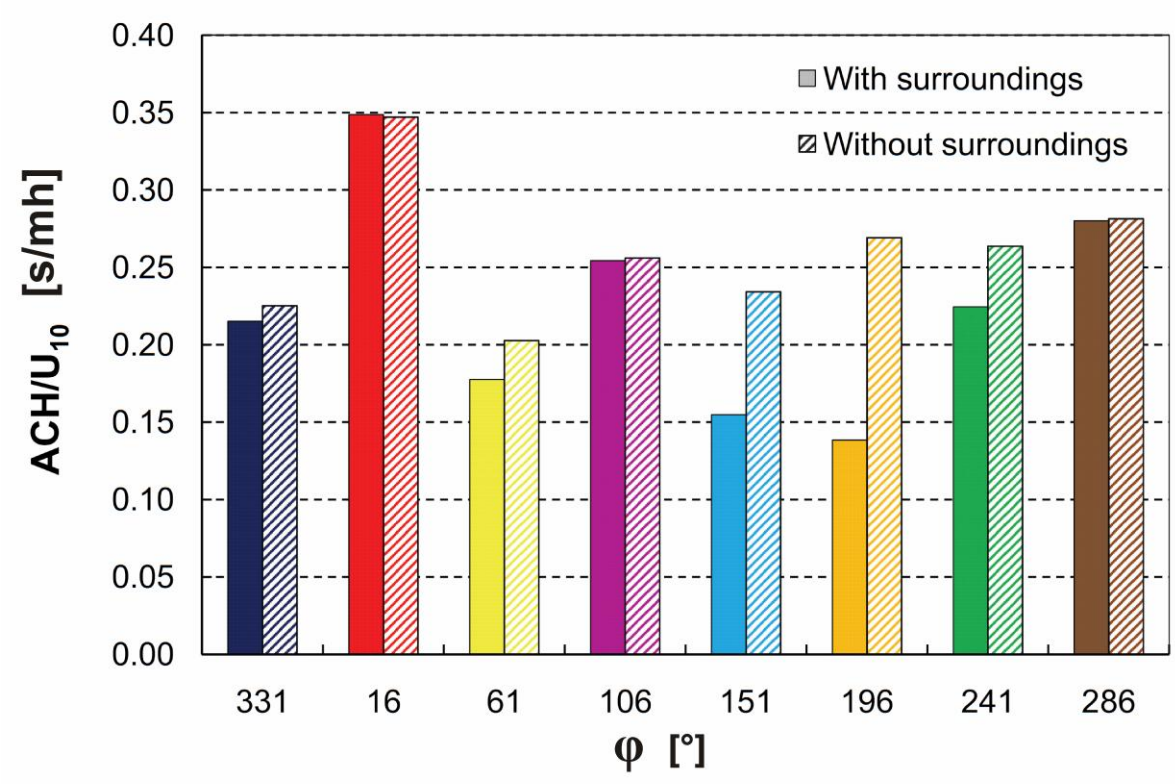

Fig. 13. ACH/U_{10} (s/mh) for eight wind directions (Fig. 10a) for Case 1 (with surrounding buildings) and for Case 2 (without surrounding buildings). The overestimation of ACH/U_{10} can be as high as 96% when the surrounding buildings are not included in the CFD model.

Tables

Table 1. Aerodynamic roughness lengths y_0 and imposed equivalent sand-grain roughness height k_S and roughness constant C_S at the bottom of the computational domain for the wind directions in this study.

φ (°)	y_0 (m)	k_S (m)	C_S (-)
16	1.0	1.4	7
61	1.0	1.4	7
106	0.5	0.7	7
151	0.5	0.7	7
196	0.5	0.7	7
241	0.5	0.7	7
286	1.0	1.4	7
331	1.0	1.4	7